The Effect of Oxygen and Carbon Dioxide Concentration on Soot Formation in Nonpremixed Flames Using Time Resolved LII Technique

Kwang Chul Oh*
Enviromental Parts R & D Center, Korea Automotive Technology Institute, 74 yongjung-Ri, Pungse-Myun, Chonan, Chungnam 330-912, Korea
Hyun Dong Shin
Department of Mechanical Engineering, Korea Advanced Institute of Science and Technology, 373-1 Guseong-dong, Yuseong-gu, Daejon 305-701, Korea

The influence of oxygen concentration and CO_2 as diluent in oxidizer side on soot characteristics was studied by Laser Induced Incandescence, Time Resolved LII and Transmission Electron Microscopy photography in non-premixed coflowing flames. Through the comparison of TEM photographs and the decay rate of LII signal, suitable two delay times of TIRE-LII method and signal sensitivity ($\Delta S_{TIRE-LII}/\Delta d_p$) were determined. The effects of O_2 and CO_2 as diluent in oxidizer side on soot formation are investigated with these calibrated techniques. The O_2+CO_2, N_2, and $[Ar+CO_2]$ mixture in co-flow were used to isolate CO_2 effects systematically. The number concentration of primary particle and soot volume fraction abruptly decrease by the addition of CO_2 to the co-flow. This suppression is resulted from the short residence time in inception region because of the late nucleation and the decrease of surface growth distance by the low flame temperature due to the higher thermal capacity and the chemical change of CO_2 including thermal dissociation. As the oxygen concentration increases, the number concentration of soot particles at the inception region increases and thus this increase of nucleation enhances the growth of soot particle.

Key Words : Soot, Laser Diagnostics (TIRE-LII, LII), Diluents

1. Introduction

Recently many combustion systems, such as EGR (Exhaust Gas Recirculation) system and oxygen enhanced combustor with CO_2 recycling, have been proposed to reduce pollutant emissions and to enhance thermal efficiency. However, the proposed systems mostly accompany drawbacks ; nitric oxide (NO_X), and soot particle emission (Angrill et al., 2000 ; Lapuerta et al. ; Shimazaki et al.). Even though there have been developments in the reduction of nitric oxide (NO_X) emission, there are still many ambiguities in soot emission due to various changes of soot characteristics (particle diameter, aggregates, the number concentration of primary particle, soot volume fraction etc) in flames. Therefore a number of investigations have focused on reducing soot emission by introducing several reduction techniques, such as using different fuels, and diluents (Zhang et al., 1992 ; Glassman, 1998 ; Gulder, 1995 ; Liu et al., 2001 ; Du et al., 1990), but it is still difficult to obtain the detailed information of their effects on soot characteristics in flames. Several experimental techniques have been de-

* Corresponding Author,
E-mail : kcoh@katech.re.kr
TEL : +82-41-559-3089; **FAX** : +82-41-559-3242
Enviromental Parts R & D Center, Korea Automotive Technology Institute, 74 yongjung-Ri, Pungse-Myun, Chonan, Chungnam 330-912, Korea. (Manuscript **Received** November 29, 2004; **Revised** December 15, 2005)

veloped to measure the soot characteristics. Optical techniques are generally considered to be the best suited for this purpose because of their non-intrusiveness, for example, light scattering (Santoro et al., 1987 ; Iuliis et al., 1998) for aggregates size, various scattering and extinction methods (Santoro and Semerjian, 1984 ; Santoro et al., 1983; Bonczyk, 1983; Tree and Foster, 1994) for measuring of both soot volume fraction and cluster structure, and multiwavelength analysis (Iuliis et al., 1998) for soot volume fraction. Unfortunately these methods have a disadvantage that it is not possible to obtain soot characteristics on the whole combustion field simultaneously because of their pointwise or line-of-sight character. Alternatively, laser induced incandescence (LII) techniques have been used successfully for two dimensional soot volume fraction measurements in a wide range combustion process (Ni et al., 1994 ; 1995 ; Shaddix et al., 1994). Recently there have been attempts in combining LII, elastic scattering, and TIRE-LII (time-resolved LII) method to measure soot characteristics simultaneously (Angrill et al., 2000 ; Will et al., 1996). Though the measurements of particle diameter with TIRE-LII is important procedure obtaining properties of aggregates, the method lacks of the consideration such as the effect of two delay times after the laser pulse and its calibration procedure.

In this study, we tried to improve the measuring technique for primary particle diameter by proper determination of two delay times. With this improved technique, we investigated the effects of oxygen concentration (25%~45%) in oxidizer side, and diluents (CO_2, Ar+CO_2) on soot characteristics such as soot volume fraction (f_v), particle size (d_p), and the number concentration of primary soot particle (N_p) in laminar nonpremixed flames.

2. Methodology

2.1 LII and soot volume fraction

The LII (Laser Induced Incandescence) method has been applied to measurement of the soot volume fraction (f_v) in many combustion systems. LII involves the heating of soot particles to temperatures above the surrounding gas temperature due to the absorption of laser energy, and subsequent detection of the blackbody radiation corresponding to the elevated soot particle temperature. If one assumes a sufficiently loose structure of soot aggregates, which may be regarded as justified with the typical fractal dimension of soot aggregates in the range 1.6-1.8, the energy balance of soot is governed by the size of primary particles according to the following Eq. (1).

$$Q_{abs}\cdot\frac{\pi d_p^2}{4}\cdot E_i-\Lambda\cdot(T-T_o)\cdot\pi d_p^2+\frac{\Delta H_V}{M}\cdot\frac{dm}{dt}-\pi d_p^2\int\varepsilon(d_p,\lambda)M_\lambda^b(T,\lambda)\,d\lambda-\frac{\pi d_p^3}{6}\rho C\frac{dT}{dt}=0 \quad (1)$$

where

Q_{abs}: Absorption efficiency
E_i : Irradiance
Λ : Heat transfer coefficient
T : Particle temperature
T_o : surrounding gas temperature
M : Molar mass of solid caron
ε : Emission coefficient
M_λ^b : Blackbody spectral radiant exitance
λ : Wavelength
ρ : Density of solid carbon
C : Specific heat of solid carbon

Melton (1984) showed that the intensity of the LII signal for a group of soot particles has a dependence on primary particle diameter as follows,

$$L_{LII}\propto N_p d_p^x,\ x=3+154/\lambda_{em} \quad (2)$$

where N_P is the number concentration of primary particles, d_p is the diameter of the primary particle, and λ_{em} is the measured wavelength. For λ_{em} between 700 nm and 400 nm, for example, the LII signal is proportional to the primary soot particle diameter raised to the power of 3.22 to 3.38, or approximately to the soot volume fraction.

Ni (1995) and Quay (1994) reported that the initial LII signal increases rapidly as laser power increases (linear region) and once laser power reaches a saturation threshold the LII signal shows a small increase or no increase (saturation region). Fig. 1 shows the intensity of the LII

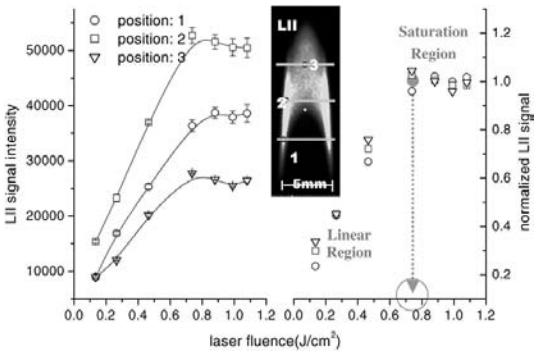

Fig. 1 The Influence of laser fluence on LII signals at three point in annular or enveloped region

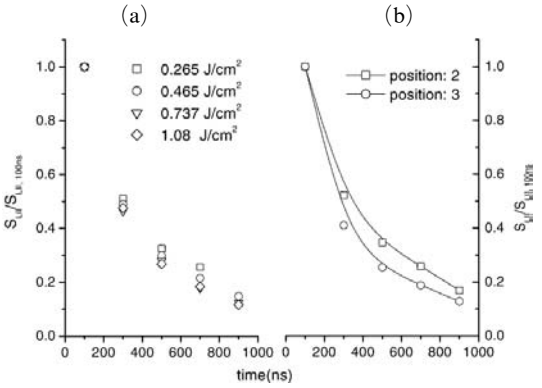

Fig. 2 The effect of laser fluence on the decay rate of LII signal

signal to the laser fluence at different positions in a flame. The intensity of the LII signal shows the same trend as the results of Ni and Quay. The laser fluence in a saturated region was used to compensate a slight inhomogeneous profile.

In this experiment, a planar laser sheet was formed using a cylindrical lens and convex lenses and the edge of the laser sheet, which is weaker in intensity, was cut off by a slit to obtain a sheet with a more uniform sheet ($I/I_{max}>0.75$ at test section). The fluence distribution of the laser sheet was confirmed with the laser Rayleigh scattering method, whose signal is proportional to laser intensity. The extinction method (Santoro et al., 1983) was used to quantify the relative soot volume fraction obtained by the LII method.

2.2 TIRE-LII and primary particle diameter

The TIRE-LII technique is based on the fact that, after laser pulse, smaller particles cool down faster than larger ones due to their larger specific surface (Santoro et al., 1983; Bonczyk, 1983; Melton, 1984). There are three paths for energy loss: vaporization, heat conduction to the surrounding gas, and radiation as shown in Eq. (1). Vaporization is a dominant path within initial period after laser pulse. Therefore the initial LII signal, within about 50 ns, is similar regardless of the diameter of the soot particle but the decay trend varies according to primary particle size in conduction dominated region. The ratio of the LII signals, measured at two different delay times, is known to be proportional to the diameter of the soot when the two delay times were determined properly (Will et al., 1998; Schraml et al., 2000).

$$S_{TIRE-LII}=S_{LII2}/S_{LII2}\propto d_p \tag{3}$$

Here, S_{LII1} is LII signal at the first delay time and S_{LII2} is LII signal at the second one. The decay curves of the LII signal after the absorption of laser energy are shown in Fig. 2. The temporal profile of LII signal changes according to a laser fluence; that is the parameter determining the initial particle temperature. As the laser fluence decreases, the cooling rate decreases due to the small temperature difference and the ratio of LII signals is high (Fig. 2(a)). But as the laser fluence gets close to saturated region, the difference is getting small. In the present study, the error of soot particle size resulted from inhomogeneous heating is approximately a maximum of (3 nm from the calibration curve (Fig. 6 (a)).

3. Experimental Details

The experimental setup consists of three parts as shown in Fig. 3. The coflowing burner was constructed to make stable flames. The inner diameter of the fuel nozzle and the co-flowing nozzle are 5 mm and 30 mm respectively. A contraction with a cut-area ratio of 1/6.5 is used

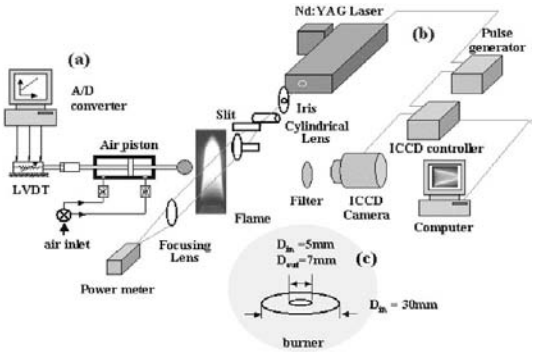

Fig. 3 Experimental apparatus: (a) Thermophoretic sampling apparatus, (b) Measuring system for LII, TIRE-LII techniques, (c) Co-flowing burner

to get a uniform velocity. The fuel is propane and its flow rate was fixed at 0.0714 l/min (V_{exit}= 6.1 cm/s). And the flow rate of the co-flow was also fixed to 20 l/min (V_{exit}=48.5 cm/s).

CO_2+O_2, $[0.61+0.39CO_2]+O_2$, and N_2+O_2 mixtures in oxidizer side were used to isolate CO_2 effects systematically. In the case of N_2 dilution, the blow-off of flame takes place when the volume fraction of oxygen is less than 19%, and in the case of CO_2, under 27% oxygen volume fraction respectively. Therefore experiments were carried out in stable flame region, the oxygen concentration, 25~45% for N_2 dilution, 30~45% for CO_2 dilution. And the adiabatic flame temperature (T_{ad}) was used as representative flame temperature. These experimental conditions and flame lengths were shown in Table 1.

The second harmonic Nd: Yag laser (λ=532 nm, I_{max}=500 mJ) was used as a laser source and its duration of the pulse (~7 ns) was very short. A laser sheet of 40 mm width was formed across the flame axis using a convex lens (f=350 mm) and a cylindrical one (f=50 mm). The edge of the laser, weaken in intensity, was cut off by an iris and a slit to get better intensity uniformity.

The detection part consisted of a filter for obtaining monochromatic signal (450 nm in LII measurement, 532 nm in Rayleigh scattering), an ICCD camera for two dimensional measurement, and pulse generator for synchronization between the laser and the ICCD camera. The camera has a 1024*256 CCD array and its spatial resolution in this experiment was about 66 μm/pixel, which was enough resolution to measure soot characteristics (d_p, N_p, f_v) in radial direction. The laser power is very important parameter in LII measurement. If excessive laser power is used, LII signal at laser incident side is smaller than the other side due to vaporization of soot. On the contrary, when insufficient laser power is used, opposite tendency occurs because of the attenuation of laser power by soot. A 0.737 J/cm^2, mean laser fluence was used in this experiment for the symmetry of soot volume fraction. 50 frames with 100 ns delay time and 50 ns gate width were accumulated in order to increase S/N ratio and flame luminosity was subtracted from LII images.

Table 1 Experimental conditions; H_f: visible flame length, T_{ad}: adiabatic flame temperature, X_{O2}: oxygen concentration in oxidizer side. *$[0.61Ar+0.39CO_2]$ is equivalent to N_2 in terms of ρC_p (298~1100K)

FUEL	Propane (=1.32 cc/sec), nozzle exit velocity= 6.7 cm/sec				
co-flow	Dilluents (N_2, CO_2, Ar) + O_2; (=20 l/min) Co-flow exit velocity=48.5 cm/sec N_2+O_2				
N_2+O_2	X_{O2}	0.25	0.30	0.35	0.40
	T_{ad} [K]	2424	2563	2663	2739
	H_f [mm]	32.4	26.2	21.1	17.9
*$0.61Ar+0.39CO_2]+O_2$	T_{ad} [K]	2346	2479	2581	2662
	H_f [mm]	31	24.04	20.1	18
CO_2+O_2	T_{ad} [K]		2197	2334	2447
	H_f [mm]		28.95	23.3	20.6

The soot sampling device as shown in Fig. 3(a) was composed of three parts, which are the part that fixes TEM grid of 3 mm (200 mesh) diameter, a potentiometer to measure the location of the TEM grid and the compressed air piston to move the grid. The moving speed of the TEM grid was controlled by the regulation of air pressure at the piston inlet. The soot was sampled by inserting a cold grid into the flame by the following procedures : rapid moving (~1 m/sec) → soot sampling (~0.2 sec, in flame) → rapid removing. The soot morphology was examined by TEM (Transmission Electron Microscopy) with a magnification of 115 K, and the soot particle size was measured by image processing with 0.73 nm/pixel resolution.

4. Result and Discussion

4.1 TEM Image and TIRE-LII method

To calibrate the relative diameter distribution obtained with TIRE-LII method the soot particles were sampled by using thermophoresis with the TEM grid. And then we obtained TEM-photographs with a magnification of 115 K, and measured primary soot particle diameters through image processing. The sampling of soot was conducted in the flames when the oxidizer mixture in co-flow was the 35% oxygen concentration with N_2 or CO_2 dilution.

Fig. 4 shows the TEM images in the case of N_2 dilution. At the location 4 mm from the nozzle, small aggregates start to appear and very small (~2 nm) soot particles, not agglomerated yet, surround the aggregates. As the progress is going on, from the nozzle to the downstream, the particle diameter becomes large and grows up to larger aggregates through the coagulation and agglomeration process. In the vicinity 14 mm from the nozzle, the diameter of particle has its largest value (~35nm) and then decrease beyond that region. The experiment with the use of CO_2 as diluents was also carried out, and the result shows similar tendency except the maximum soot particle diameter is 26 nm.

TIRE-LII method was applied to the flame under the same condition. As explained previously, the intensity of TIRE-LII signal is proportional to the size of primary particle. Therefore the planar distribution of soot particle size

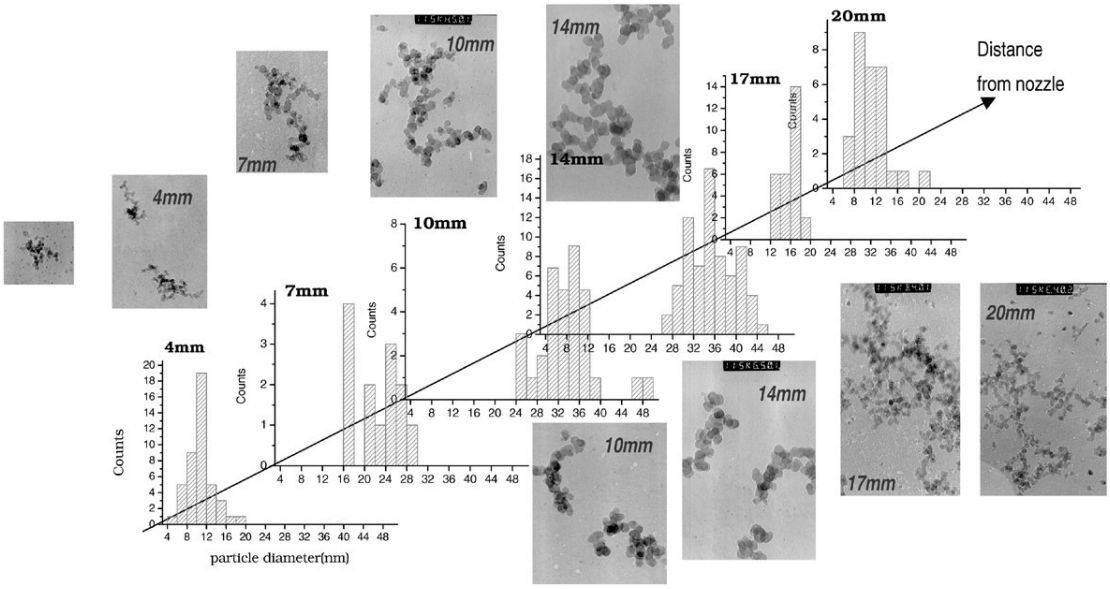

Fig. 4 TEM photographs of soot aggregates and particle size distribution at the position of maximum soot volume fraction along the axial direction in the N_2+O_2 (X_{O2}=0.35) co-flow flame with magnification of 115,000

can be obtained if the calibration between the diameter and the signal intensity is properly performed. Fig. 6(a) shows the correlation between the particle diameter and the signal intensity obtained with TEM and TIRE-LII method respectively. The relation between particle diameter and TIRE-LII signal has a linear tendency that has a slope $(\Delta d_p/\Delta S_{TIRE-LII})$ and an intercept which is minimum measurable diameter. The intercept increases according to the second delay time after laser pulse because the LII signal of small particle decreases rapidly to the noise level. Fig. 5(a) shows the minimum measurable particle diameter as the second delay time increases. The sensitivity of TIRE-LII signal to the particle diameter according to second delay time is shown in Fig. 5(b). The sensitivity is defined as follows

$$S=\frac{1}{S_{TIRE-LII,\max}}\cdot\frac{\Delta S_{TIRE-LII}}{\Delta d_p} \qquad (4)$$

where, $S_{TIRE-LII,\max}$ is TIRE-LII signal at 10 mm (primary particle size=34 nm) in N_2 diluent case. The increase of the second delay time causes the sensitivity of TIRE-LII to increase. Therefore, if the second delay time is close to the first delay time, measurable particle size becomes small, but the sensitivity to the size of particles decreases. On the contrary, when the second delay time is retarded, there is a drawback that measurable particle size increases (when 700 ns, 12.5 nm). Suppose the situation that the calibration was conducted at one diameter, TIRE-LII will overestimate soot particle diameter in the case of larger diameter than the calibrated diameter. In the opposite case, the diameters measured with TIRE-LII will be smaller than true diameter. In this work, the ratio between the signals at two different delay times (100 ns and 550 ns) were used to measure the sizes of particle (minimum measurable diameter : 7.4 nm). The calibration curve between TEM images and TIRE-LII signals is shown in Fig. 6(a) and the primary soot particle diameter in axial direction in Fig. 6(b). The soot particle size measured by laser method is in good agreement with that measured by TEM photographs.

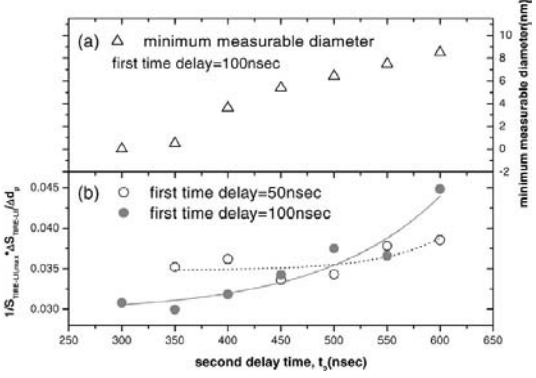

Fig. 5 The sensitivity of TIRE-LII signal and minimum measurable diameter according to two delay times after laser pulse

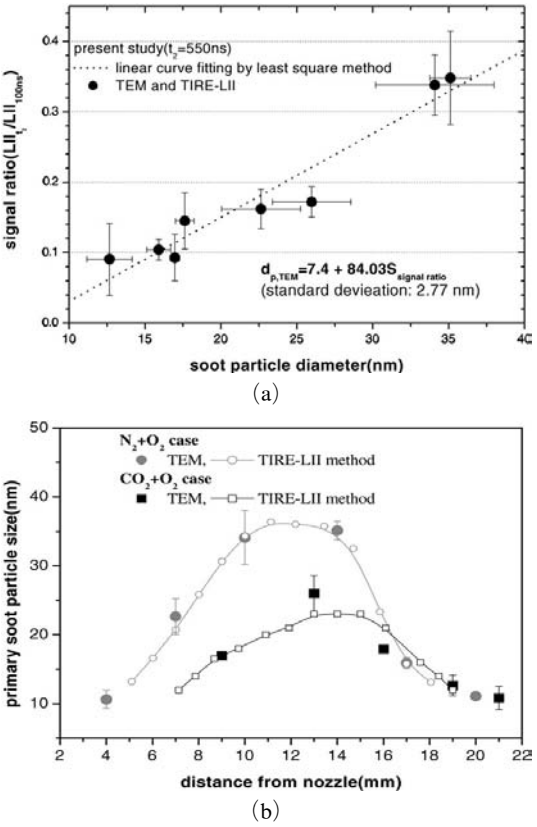

Fig. 6 Calibration curve between TEM photographs and TIRE-LII technique in CO_2, N_2+O_2 coflowing condition (X_{O2}=0.35) (a) calibration curve between TEM images and TIRE-LII signal, (b) Primary soot particle diameter above the nozzle from the TEM photographs and laser technique

4.2 The effects of oxygen concentration and diluents

The characteristics of soot according to oxygen concentration and diluents were measured by using combined LII and TIRE-LII method. Fig. 7 shows the distributions of primary soot particle (d_p), volume fraction (f_v), and the number concentration of primary particle (N_p) at 30% oxygen concentration in co-flow. In the case of using CO_2 as diluents instead of N_2, the primary particle size and soot volume fraction abruptly decrease while the number concentration of primary particles increase at the enveloped region. At the inception region, the reduction of Np causes the agglomerate process to slow down due to the decrease of the collision frequency, thus it could be deduced that the size of primary particles within aggregate is smaller than that of N_2 diluents case. The suppression of soot volume fraction in CO_2 diluted co-flow is due to low flame temperature (thermal effects, Table 1) and chemical effects (Gulder, 1995; Du, 1990). The proper CO_2 and Ar mixtures equivalent to N_2 case in terms of specific heat capacity (ρC_p) in 298K~1100K was used to isolate the thermal effects of CO_2. The flame length is similar and the difference of adiabatic flame temperatures is about 90K (see Table 1) between N_2 and Ar+CO_2 diluents. Comparing Fig. 7(a) with Fig. 7(c), the number concentration of primary particles (N_p=0.37#/μm^3) of CO_2 and Ar mixture is lower than that of N_2 (N_p=0.77#/μm^3) case in the soot inception region. The change of Np can be explained by the chemical effects of CO_2 that includes the reduction of flame temperature (90K) and the increase of OH via $CO_2+H \leftrightarrow CO+OH$ chemical reaction (Angrill, 2000; Liu, 2001). And these changes also retard the growth of soot particle size. Fig. 8 shows the maximum values of d_p, N_p and the integrated soot volume fraction (f_{Iv}) in axial direction at X_{O2}=0.25 and 0.4. At Z/H_f=0.3, the soot particle size grows up while the number concentration of primary particles decreases. Through this process, small soot particles grow to large ones or to chains. The number concentration of primary particles

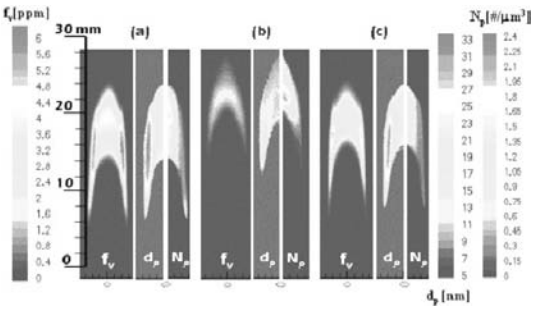

Fig. 7 Soot volume fraction, primary particle size, and the number concentration of primary particles distribution in 30% oxygen volume fraction, (a) N_2+O_2, (b) CO_2+O_2, (c) [0.61Ar+0.39CO_2]+O_2 case in co-flow

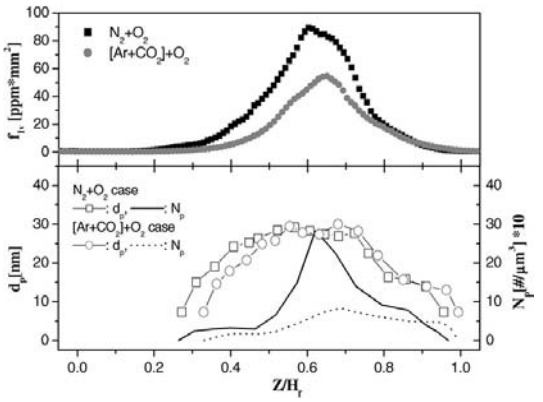

(a) X_{O2}=0.25

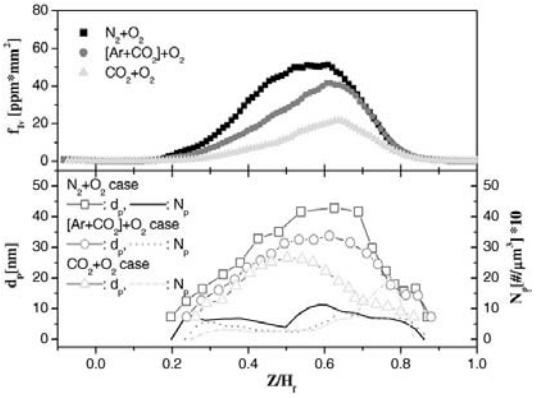

(b) X_{O2}=0.4

Fig. 8 Integrated soot volume fraction (f_{Iv}), maximum primary particle diameter (d_p), and the maximum number concentration of primary particles along the flame in X_{O2}=0.25 and X_{O2}=0.40

increases again at Z/H_f=0.6 and has the maximum value in this region (enveloped region). According to the increase of the oxygen concentration in co-flow, the increase of the number concentration of soot particles at the inception region causes the growth rate of particle to increase. The $d_{p,max}$, $f_{v,max}$, $f_{Iv,max}$, and $N_{p,max}$ according to the oxygen concentration and diluents are shown in Fig. 9. As the oxygen concentration in co-flow increases, the local maximum soot volume fraction ($f_{v,max}$) increases but the maximum of integrated soot volume fraction ($f_{Iv,max}$) decreases because the flame volume containing soot is small due to enhanced oxidation rate by OH, O_2 species. And the soot particle size is about 35 nm (N_2), 29 nm ($0.61Ar+0.39CO_2$) and 22 nm (CO_2), and there is variation of a few nm according to the oxygen concentration in co-flow.

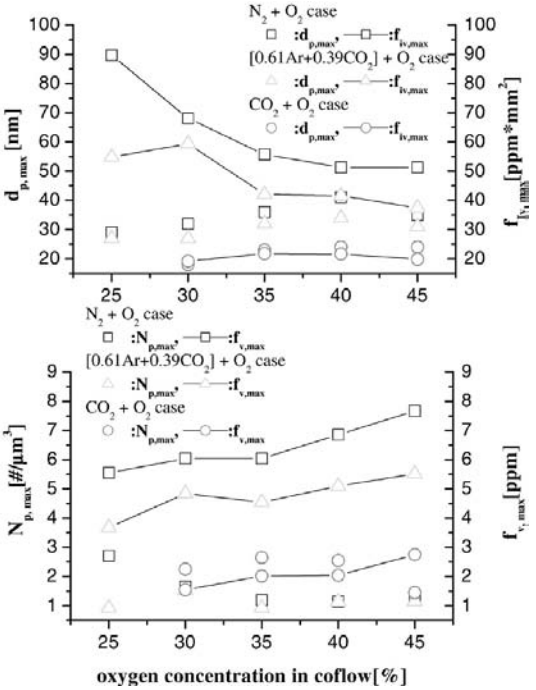

Fig. 9 Maximum soot volume fraction (f_v), maximum integrated soot volume fraction (f_{Iv}), maximum primary particle diameter (d_p), and the maximum number concentration of primary particles varying the oxygen concentration

5. Concluding Remark

The influence of oxygen concentration and diluents in oxidizer side on distribution of f_v, d_p, and N_p was studied by combined LII and TIRE-LII method in propane non-premixed flames. Two delay times, 100 ns and 550 ns, of TIRE-LII method were determined for measuring 8～40 nm particle size by comparing the particle diameters obtained by TEM and TIRE-LII signal intensity respectively. The number concentration of primary particles in the case of [0.61Ar+0.39CO_2] which is equivalent to N_2 in terms of ρC_p in 298～1100K to isolate thermal effect is lower than that of N_2 case at soot inception region by the chemical effects of CO_2 that includes the reduction of flame temperature (90K) and the increase of OH via $CO_2+H \leftrightarrow CO+OH$ chemical reaction. As the oxygen concentration in co-flow increases, the local maximum soot volume fraction ($f_{v,max}$) increases but the maximum of integrated soot volume fraction ($f_{Iv,max}$) decreases because the flame volume containing soot is small due to enhanced oxidation rate. Although there are uncertainties of flame temperature and chemical composition, the present experimental investigations supply detailed information on soot characteristics in flames.

Acknowledgments

This research was supported by the Korea Science and Technology Foundation (KOSEF) through the Combustion Engineering Research Center (CERC) and Ministry of Commerce, Industry and Energy.

References

Angrill, O., Geitlinger, H., Streibel, T., Suntz, R. and Bockhorn, H., 2000, "Influence of Exhaust Gas Recirculation on Soot Formation in Diffusion Flames," Proc. Combust. Instit. 28, pp. 2643.

Bonczyk, P. A., 1983, "In-situ Optical Measurement of Additive Effects on Particulates in a Sooting Diffusion Flame," Combust. Flame 51,

pp. 219.

Du, D. X., Axelbaum, R. L. and Law, C. K., 1990, "The Influence of Carbon Dioxide and Oxygen as Additives on Soot Formation in Diffusion Flames," Proc. Combust. Instit. 23, pp. 1501.

Glassman, Irvin, 1998, "Sooting Laminar Diffusion flames : Effect of Dilution, Additives, Pressure, and Microgravity," Proc. Combust. Inst. 27, pp. 1589.

Gulder, Ö. L., 1995, "Effects of Oxygen on Soot Formation in Methane, Propane, and n-Butane Diffusion Flames," Combust. Flame 101, pp. 302.

Iuliis, S. De, Cignoli, F., Benecchi, S. and Zizak, G., 1998, "Investigation of the Similarity of Soot Parameters in Ethylene Diffusion Flames with Different Heights by Extinction/Scattering Technique," Proc. Combust. Instit. 27, pp. 1549.

Iuliis, S. De, Barbini, M., Benecchi, S., Cignoli, F. and Zizak, G., 1998, "Determination of the Soot Volume Fraction in an Ethylene Diffusion Flame by Multiwavelength Analysis of Soot Radiation," Combust. Flame 115, pp. 253.

Lapuerta, M., Salavert, J. M. and Domenech, C., "Modelling and Experimental Study about the Effect of Exhaust Gas Recirculation on Diesel Engine Combustion and Emission," SAE paper 95-0216.

Liu, F., Guo, H., Smallwood, G. J. and Gulder, O. L., 2001, "The Chemical Effects of Carbon Dioxide as an Additive in an Ethylene Diffusion Flame : Implications for Soot and NOx Formation," Combust. Flame 125, pp. 778.

Melton, L. A., 1984, "Soot Diagnostics Based on Laser Heating," Appl. Opt.23, pp. 2201.

Ni, T., Gupta, S. B. and Santoro, R. J., 1994, "Suppression of Soot Formation in Ethane Laminar Diffusion Flames by Chemical additives," Proc. Combust. Instit. 25, pp. 585.

Ni, T., Pinson, J. A., Gupta, S. and Santoro, R. J., 1995, "Two-dimensional Imaging of Soot Volume Fraction by the Use of Laser-Induced Incandescence," Appl. Opt. 34, pp. 7083.

Quay, B., Lee, T. W., Ni, T. and Santoro, R. J., 1994, "Spatially Resolved Measurements of Soot Volume Fraction Using Laser-Induced Incandescence," Combust. Flame 97, pp. 384.

Santoro, R. J., Yen, T. T., Horvath, J. J. and Semerjian, H. G., 1987, "The Transport and Growth of Soot Particles in Laminar Diffusion Flames," Combust. Sci. and Tech. 53, pp. 89.

Santoro, R. J. and Semerjian, H. G., 1984, "Soot Formation in Diffusion Flames : Flow Rate, Fuel Species and Temperature Effects," Proc. Combust. Instit. 20, pp. 997.

Santoro, R. J., Semerjian, H. G. and Dobbins, R. A., 1983, "Soot Particle Measurements in Diffusion Flames," Combust. Flame 51, pp. 203.

Schraml, S., Dankers, S., Bader, K., Will, S. and Leipertz, A., 2000, "Soot Temperature Measurements and Implications for Time-Resolved Laser-Induced Incandescence (TIRE-LII)," Combust. Flame 120, pp. 439.

Shaddix, C. R., Harrington, J. E. and Smyth, K. C., 1994, "Quantitative Measurements of Enhanced Soot Production in a Flickering Methane/Air Diffusion Flame," Combust. Flame 99, pp. 723.

Shimazaki, N., Hatanak, H., Yokota, K. and Nakahira, T., "Study of Diesel Combustion Process under the Condition of EGR and High-Pressure Fuel Injection with Gas Sampling Method," SAE paper 96-0030.

Tree, D. R. and Foster, D. E., 1994, "Optical Soot Particle Size and Number Density Measurements in a Direct Injection Diesel Engine," Combust. Sci. and Tech. 95, pp. 313.

Vander Wal, R. L., Ticich, T. M. and Stephens, B., 1999, "Can Soot Primary Particle Size be Determined Using Laser-Induced Incandescence?," Combust. Flame 116, pp. 291.

Will, S., Schraml, S. and Leipertz, A., 1996, "Comprehensive Two Dimensional Soot Diagnostics Based on Laser-Induced Incandescence (LII)," Proc. Combust. Instit. 26, pp. 2277.

Will, S., Schraml, Bader, S. K. and Leipertz, A., 1998, "Performance Characteristics of Soot Primary Particle Size Measurements by Time-Resolved Laser-Induced Incandescence," Appl. Opt. 37, pp. 5647.

Zhang, C., Atreya, A. and Lee, L., 1992, "Sooting Structure of Methane Counterflow Diffusion Flames with Preheated Reactants and Dilution by Products of Combustion," Proc. Combust. Instit. 24, pp. 1049.